Article ID: 1003－6326(2003)01－0103－08

Mechanism of removing inclusions from molten aluminum by stirring active molten flux①

ZHOU Ming(周 鸣), LI Ke(李 克), SUN Bao-de(孙宝德), SHU Da(疏 达),
NI Hong-jun(倪红军), WANG Jun(王 俊), ZHANG Jiao(张 佼)
(School of Materials Science and Engineering, Shanghai Jiaotong University, Shanghai 200030, China)

Abstract: Removal of inclusions from industrial pure molten aluminum(A01) by stirring active molten flux was studied. Wettability of nonmetallic inclusions in the molten aluminum was worse than that in active molten flux. According to the surface renewal model, the inclusions were easily transferred into molten active flux from fine aluminum droplets and then reacted chemically when molten aluminum was dispersed into fine aluminum droplets in stirring active molten flux. Tensile tests show that tensile strength of purified tensile sample(as-cast) increases by 8.59%. SEM photographs show that the fracture cracks of purified tensile sample are homogeneous, and the dimples are small and homogeneous. From metallographs and statistic results of Leco analysis software, it is found that the quantities and sizes of the inclusions in purified sample are obviously fewer and smaller than in unpurified tensile sample(as-cast).

Key words: flux; inclusion; stirring; molten aluminum; surface renewal kinetic model
CLC number: TG 146.21 **Document code:** A

1 INTRODUCTION

Molten aluminum is so active that it easily reacts chemically with H_2O(gaseous state) in melting operation, and alumina inclusions(Al_2O_3) and hydrogen gas(H_2) are produced. However, some non-oxidative inclusions, such as TiB_2, Al_4C_3, $MgAl_2O_4$, are also produced during the electrolytic process. Aluminum products containing these nonmetallic inclusions will probably exhibit poor toughness properties in service. Therefore, purifying molten aluminum is one of the most important processes for improving quality of aluminum product[1].

Molten flux removing inclusions and degassing have the advantages of simple technology and low cost, which can satisfy requirements of industrial production with general methods of purifying molten aluminum. The inclusions in molten aluminum should be removed to be as rarely as possible in the electronic industry, the aviation industry, the building materials industry and the automobile industry. But the requirements are not satisfied with present methods of flux removing inclusion. So, it is necessary to research and develop new style of removing inclusions and degassing.

At the present time, the fluxes including fluoride, chlorine salt and carbonate are widely used in aluminum processing industry, and mixed salts are put into molten aluminum after being dried with bake oven and mixed with ball milling. The mixed salts can remove some inclusions when they are melted in molten aluminum. However, efficiency of removing inclusion is not notable due to the inadequate contact with molten aluminum[2]. Moreover, these salts are mixed inadequately using general process of ball milling, some components in mixed salts can not form low melting point eutectic. Their melting points are higher than that of molten aluminum, and then some new inclusions are produced.

FU et al[3-7] purified the industrial pure aluminum with the reactive flux. KCl and NaCl are main components in reactive flux, besides small quantity of fluoride, carbonate, sulfate and fusing agent are used. The aluminum ingots are put on the mixed salts, and the molten aluminum passes through the layer of the melting flux when aluminum ingots and mix salts are melted. Some inclusions on the surface of the molten aluminum can be removed. But the inclusions in the middle of the molten aluminum can not be removed because they have few chances to contact with molten fluxes.

Surfaces of the inclusions are covered by liquid aluminum because inclusions disperse in molten aluminum. From thermodynamic analysis, it is found that inclusions tend to transfer from molten aluminum to molten flux, but liquid metallic film on the surface of the inclusions hinders inclusions contacting with molten flux. If the thickness of the liquid aluminum film is reduced or the liquid aluminum film is torn up, the inclusions can transfer into stirring molten flux from the interface between molten alu-

① **Foundation item:** Project(G1999064900) supported by National Key Fundamental Research and Development Program of China
Received date: 2002－01－05; **Accepted date:** 2002－04－15
Correspondence: Prof. SUN Bao-de; E-mail: jdzhm@sohu.com, bdsun@sjtu.edu.cn

minum and flux[8-15].

The object of this study is to investigate the removal of inclusions after molten aluminum being dispersed into fine aluminum droplets in stirring molten active flux and to explain the mechanism of removing inclusions using thermodynamic theories and surface renewal kinetic model.

2 EXPERIMENTAL

The industrial pure aluminum ingot(A01) was used in experiment, and the melting equipment was a 12 kW graphite crucible and electric resistance furnace. The commercial and chemical pure active fluxes were used in experiments, and only the fresh flux was used for each new purifying. The components of active flux are listed in Table 1.

Table 1 Components of active melting flux (mass fraction, %)

Sample No.	NaCl	KCl	$NaAlF_6$	NaF	$CaCl_2$	$NaCO_3$	KCO_3	KBF_4
F_1	35	35	10	6	4	3	3	4
F_2	30	30	18	10	7	0	0	5

The purifying process began with preparing two graphite crucibles in the electric resistance furnace: one graphite crucible was filled with 300 g active fluxes, and the other was filled with 900 g industrial pure aluminum ingot and covered by 150 g active fluxes on the surface. After the fluxes and the aluminum ingot being melted, molten aluminum was added into the molten active flux being stirred with an electric agitator(JB50-D type). The purified molten aluminum was poured into a die preheated at 220 ℃ after being held for 10 min at melting furnace. Table 2 shows the detailed processing parameters of the stirring flux purification. Fig. 1 and Fig. 2 represent the primary and final states of the molten aluminum being purified by stirring molten flux and the purifying facilities.

Table 2 Detailed process of stirring flux purification

Sample No.	Melt temp./℃	Rotational speed/($r \cdot min^{-1}$)	Purification times	Adding quantity of flux/g	Covering flux/g
S_0	720	0	0	0	150
S_{F11}	720	500	1	300	150
S_{F12}	720	500	2	600	
S_{F21}	720	500	1	300	150
S_{F22}	720	500	2	600	

Notice: the flux F_1 was used to purify S_{F11} and S_{F12}, the flux F_2 was used to purify S_{F21} and S_{F22}. The final Arabic figures in subscript of sample No. represent purification times.

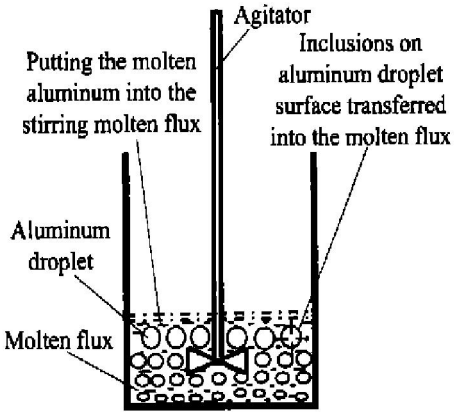

Fig. 1 Primary state of molten aluminum put into stirring molten flux

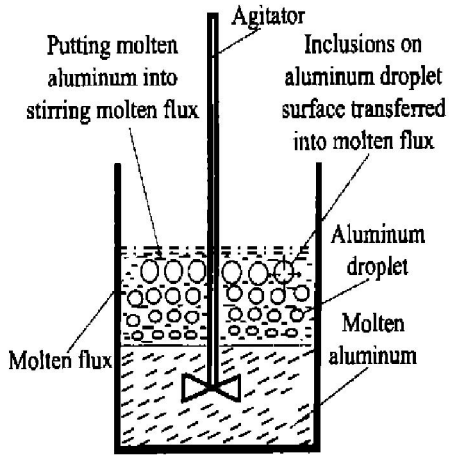

Fig. 2 Final state of molten aluminum put into stirring molten flux

The phase components of pulverous active fluxes were detected by X-ray diffraction(Rigaku Dmax-rC), and the components of pulverous active fluxes were detected by electron probe combined with scanning electron microscopy(EPMA-8705QH_2 + INCA, energy spectrometer); the as-cast tensile samples(d 11.25 mm × 100 mm) were tested by a hydraulic universal material testing machine(type WE-300A); the fracture pattern of tensile sample was observed by scanning electron microscopy (SEM, EDAX-S-520); the impurity elements of the tensile samples were detected by inductive couple plasma emission spectroscopy(ICP-AES, IRIS-1000 type). On the other hand, the shapes and sizes of the inclusions on metallographic specimens were observed by an image analysis apparatus(OLYMPUS PME3), and the quantities of the inclusions were counted by a Leco image analysis software.

3 RESULTS

Fig. 3 shows the X-ray diffraction spectra of unused and solidified pure active flux and used and solidified molten active flux. The inclusions are dissolved in the molten active flux and are not

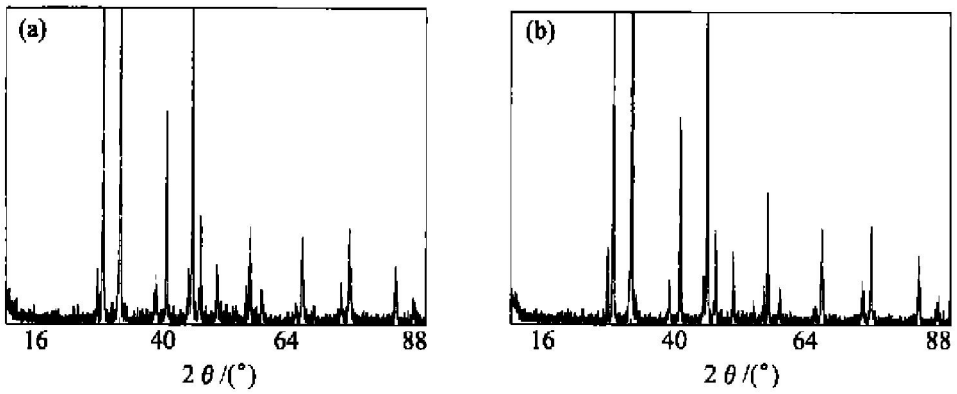

Fig. 3 X-ray diffraction spectra of pure active flux(a) and used active flux(b)

detected by X-ray diffraction spectra because the contents of the inclusions are lower than the detective limit(1%) of X-ray diffraction. Therefore, X-ray diffraction spectrum in Fig. 3(a) is the same as that in Fig. 3(b). The electron energy spectrum of the components of solidified active flux used to purify molten aluminum is shown in Fig. 4, but element oxygen can not be detected by electron probe in small area of high fluorine content($AlOF_2^-$) because the inclusions are dissolved in the molten active flux and their contents are lower than the detective limit(0.1%) of the electron probe. Fig. 5 shows the X-ray diffraction spectrum of used and solidified KCl-NaCl flux, and the inclusions in molten aluminum have been detected by X-ray diffraction because the molten KCl-NaCl flux hardly reacts chemically with the inclusions(Al_2O_3). The reaction equation is as follows:

$$Al_2O_3 + AlF_6^{3-} \rightarrow 3AlOF_2^- \quad (1)$$

$$Al_2O_3 + 4AlF_6^{3-} \rightarrow 3(AlF_3-O-F_3Al) + 6F^- \quad (2)$$

The inclusions in molten flux can not reenter the molten aluminum during purifying process because the inclusions react chemically with molten active flux. On the contrary, the inclusions in molten KCl-NaCl flux may reenter the molten aluminum.

The tensile sample S_0 is the original sample unpurified by the stirring molten flux. By contrast, the tensile strength of tensile sample S_{11} increases by 4.85%, and the tensile strength of tensile sample S_{12} increases by 8.59% after being purified for one and two times. According to data in Table 3, it is clear that the tensile strength of the tensile sample further increases with the increase of purifying times, but the elongation decreases slightly.

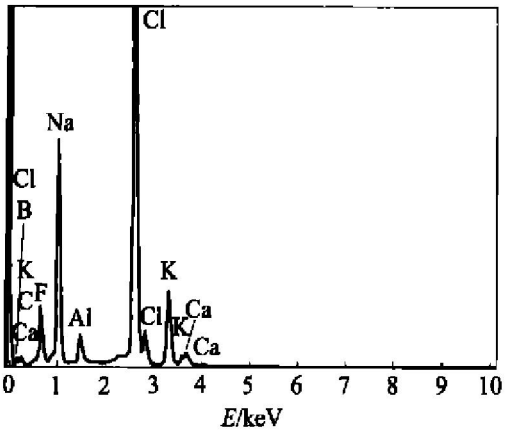

Fig. 4 Electron spectrum of components of high fluorine content area with electron probe analysis

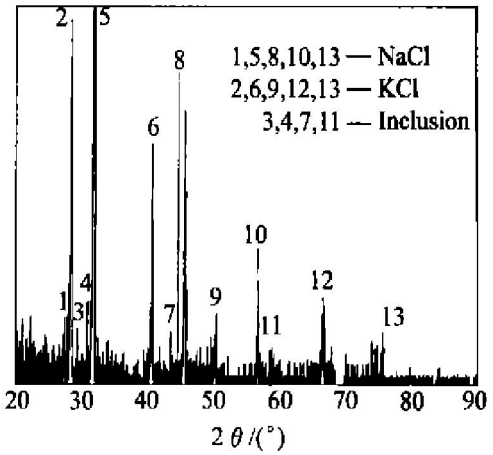

Fig. 5 X-ray diffraction spectrum of flux after fourth purifying

Table 3 Tensile strength and elongation of tensile samples(average)

Sample No.	Tensile strength/MPa	Elongation /%	Strength increment/%
S_0	70.45	45.00	
S_{11}	73.87	44.17	4.85
S_{12}	76.50	43.33	8.59
S_{21}	73.61	44.33	4.49
S_{22}	76.50	43.33	8.59

The contents of the trace impurity elements in the tensile sample S_{F12} are slightly higher than that of the tensile sample S_0 according to Table 4.

The fracture pattern of the tensile sample S_0 is shown in Fig. 6(a). The fracture is quite inhomogeneous and dimples are large and non-homogeneous. Fig. 6(b) shows

the fracture pattern of sample S_{FI2}. It can be seen according to the SEM photographs that the dimples are very fine and homogeneous, and the ductile fracture is produced easily because the inclusions are decreased after being purified by molten flux.

Table 4 Analysis of impurity elements for tensile sample with ICP-AES(mass fraction, %)

Sample No.	Pb	B	Ca	Cr
S_0	0.041 4	0.027	0.005 8	0.003 3
S_{F12}	0.041 7	0.044	0.014	0.015
Sample No.	Fe	Mg	Na	Si
S_0	0.089 9	0.002 8	0.003 3	0.045 6
S_{F12}	0.077 9	0.004 7	0.005 6	0.051 6

The size and statistical distribution of the non-metallic inclusions are observed and counted respectively with image instrument and Leco image analytic software. Fig. 7 (a) and Fig. 8(a) show metallographic photographs of tensile samples S_0 and S_{FI2} respectively. By contrast, the inclusions in Fig. 7(a) are fewer than that in Fig. 8(a). Fig. 7(b) and Fig. 8(b) show the metallographs of the tensile samples S_0 and S_{F12}, respectively. A small quantity of 20 μm inclusions is found by the metallograph of tensile sample S_0 in Fig. 8(a), and the size of the inclusions of tensile sample S_{F12} is mostly 7 μm in Fig. 8(b).

The distribution of the nonmetallic inclusions is counted with Leco image analytic software by collecting eighty fields of view on metallographic specimen. The

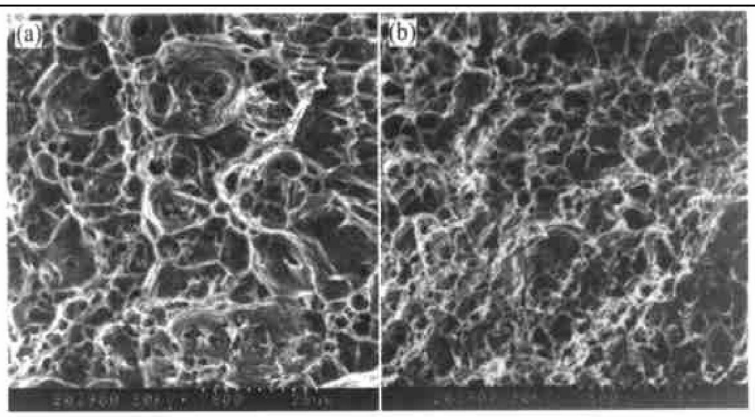

Fig. 6 Fractographs of tensile sample S_0(a) and sample S_{F12}(b)

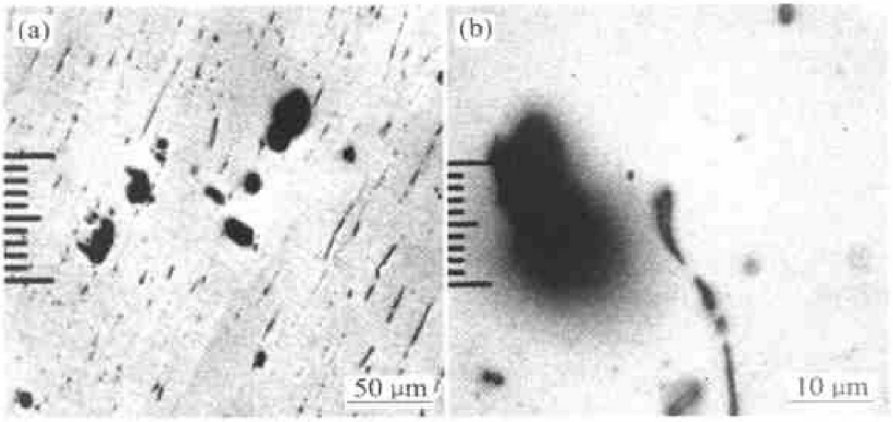

Fig. 7 Metallographic photograph of tensile samples S_0

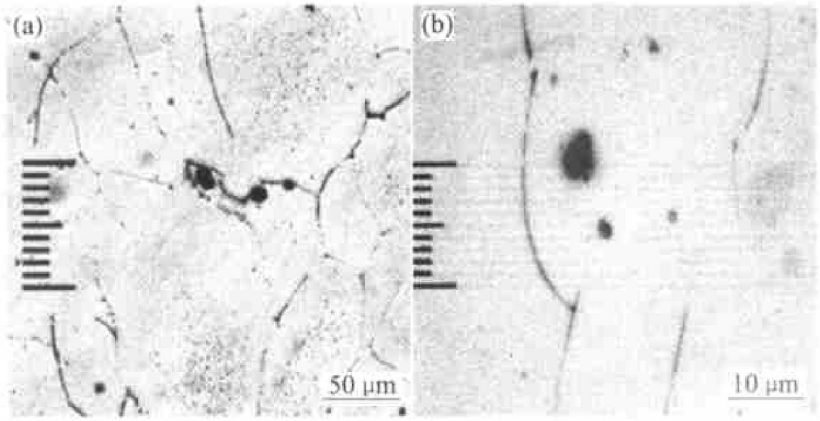

Fig. 8 Metallographic photograph of tensile samples S_{F12}

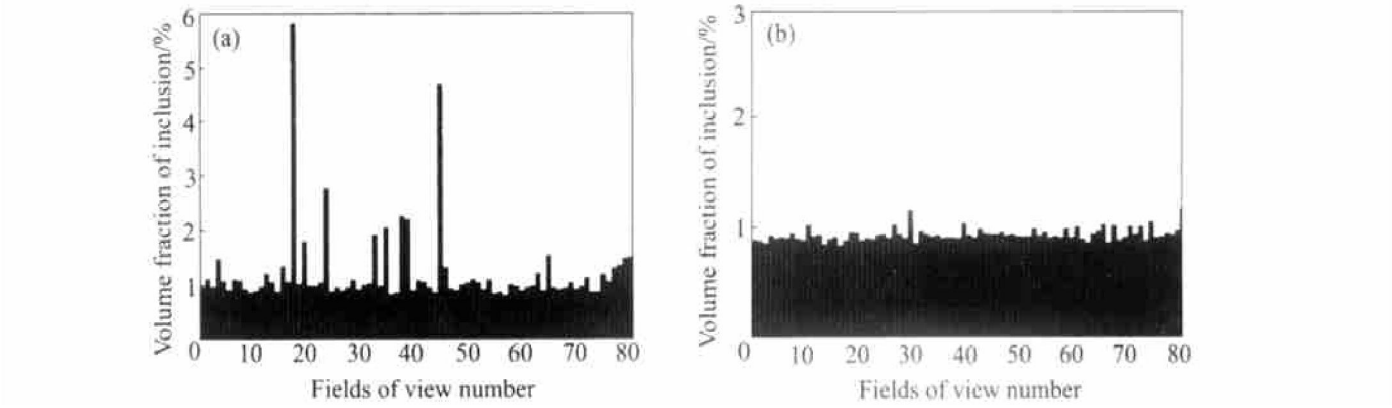

Fig. 9 Statistical distribution of tensile sample S_0(a) and tensile sample S_{F12}(b)

area of every field of view and the total area are 0. 006 1 mm^2 and 0. 488 mm^2 respectively. Fig. 9(a) shows that the maximum and minimum volume fractions of the inclusions in tensile sample S_0 are 5. 83% and 0. 83 % respectively, and the average volume fraction is 1. 23%. The maximum and minimum volume fractions of the inclusion in tensile sample S_{F12} are 1. 15% and 0. 83 % respectively in Fig. 9(b), and the average volume fraction is 0. 92%. By contrast, the nonmetallic inclusions of the sample S_{F12} are smaller and fewer than that of sample S_0.

4 DISCUSSION

4. 1 Thermodynamic analysis of melting flux removing inclusion[16-21]

Thermodynamically, the wetting angle($\theta_{MI} > 90°$) of the nonmetallic inclusions in the molten aluminum is larger than that in the flux, and the surface tension is also larger than that in the flux , but the stability is worse than that in the flux. Therefore, the inclusions tend to be transferred from the molten aluminum into the flux. Thermodynamic expression of the molten flux removing inclusions are shown as follows[16-21]:

$$\Delta G = \gamma_{IF} - \gamma_{MF} - \gamma_{IM} \quad (3)$$

$$\gamma_{IG} = \gamma_{FG}\cos\theta_{IF} + \gamma_{IF},$$

$$\gamma_{IG} = \gamma_{MG}\cos\theta_{IM} + \gamma_{IM} \quad (4)$$

$$\Delta G = -\gamma_{FG}\cos\theta_{IF} + \gamma_{MG}\cos\theta_{MI} - \gamma_{MF} \quad (5)$$

where ΔG —Gibbs free energy of the inclusion-molten aluminum-flux system; γ_{MF} —surface tension between the molten aluminum and the flux; γ_{IF} —surface tension between the inclusion and the flux; γ_{IM} —surface tension between the inclusion and molten aluminum; θ_{MI} —wetting angle between the molten aluminum and inclusion(> 90°); θ_{IF} —wetting angle between the inclusion and flux (< 90°); γ_{IG} —Surface tension between the inclusion and gas; γ_{FG} —surface tension between the flux and gas; γ_{MG} —surface tension between the molten aluminum and gas.

Thermodynamic conditions for the flux purifying are shown as follows: $\Delta G < 0$, the inclusions are non-wetted in the molten aluminum ($\theta_{MI} > 0°$ or $\cos\theta_{MI}$) in Eqn. (5). The larger γ_{MF} between the molten aluminum and the flux is, the smaller ΔG and easier the inclusions could be removed by the molten flux.

4. 2 Analysis of kinetic model of melting flux removing inclusion

Shear force produced by the rotary of the agitator makes the molten aluminum disperse into the fine aluminum droplets. The fine aluminum droplets can pass through the layer of the stirred flux because the density of the fine aluminum droplet is larger than that of the molten flux, which is reduced gradually from the melting flux top to the melting flux bottom due to the action of the shear force. In addition, the surfaces of both the aluminum droplet and molten flux are renewed again and again because they are in swirling turbulent flow and the rotary melting flux make aluminum droplet revolve. Therefore, the inclusions in the molten aluminum and the aluminum droplet can be transferred onto the surface of the aluminum droplets. The surface renewal model of the aluminum droplet in rotary melting flux is shown in Fig. 10, and Fig. 11 shows the diffusion process of inclusions in interface.

In the surface renewal model[22-26] or the penetr-

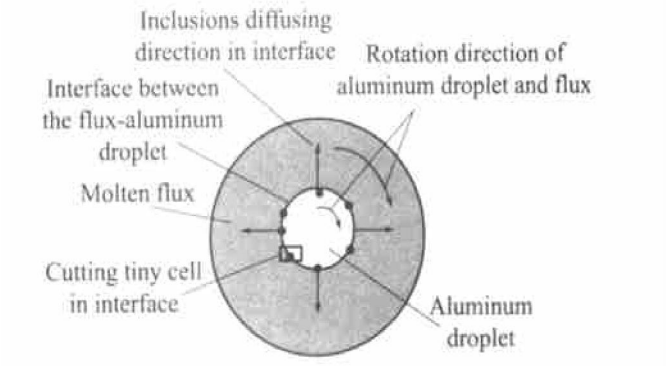

Fig. 10 Inclusions on surface of aluminum droplet diffusing into molten flux

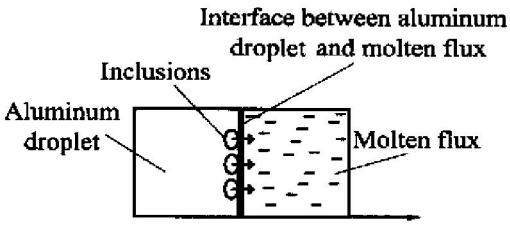

Fig. 11 Tiny cell of enlarged interface between aluminum droplet and molten flux

ation—surface renewal model, give that the fluid surface is refreshed continuously by new fluid, the two-phase fluid will be under the turbulent condition and extend to the phase interface. So the inclusions will be transferred onto the surface of the aluminum droplets, and then penetrate from the interface into molten flux layer.

The average mass transfer formula of the inclusion is obtained according to the surface renewal model of the aluminum droplet in melting flux.

$$\overline{n}_i = (C_i - C_0)\sqrt{D_d s} \tag{6}$$

So, mass transfer formula coefficient of the inclusion is obtained as follows:

$$k_c = \sqrt{D_d s} \tag{7}$$

where D_d is diffusion coefficient of the inclusion, s is the ratio of surface renewal.

The surface renewal rate s is proposed in the surface renewal dynamic model, which represents the percentage of the renewed surface in the total surface areas in unit time [1/s] or [$m^2/m^2 \cdot s$].

From Eqn. (6), the rate of mass transfer k_c is directly proportional to $s^{1/2}$, and the ratio of surface renewal s has relation with rotating speed. The higher the rotate speed of the agitator is, the larger the value of s and the rate of mass transfer are.

The ratio of surface renewal s is expressed by

$$s = \frac{S_f}{S_a \cdot t} = \frac{4\pi r^2}{4\pi r^2 \cdot t} = \frac{2\pi r}{2\pi r \cdot t} = \frac{2\pi r}{t} \times \frac{1}{\pi d_a} = \frac{v_a}{\pi d_a} \tag{8}$$

where S_f is surface area of molten flux contacting with aluminum droplet, S_a is surface area of aluminum droplet, v_a is rotary speed of aluminum droplet, r is radius of aluminum droplet, d_a is diameter of aluminum droplet, t is rotary time of a circuit of aluminum droplet.

By substituting Eqn. (8) into Eqn. (7), it can be obtained:

$$k_c = (D_d v_a / \pi d_a)^{1/2} \tag{9}$$

From Eqn. (9), mass transfer coefficient of the inclusion is increased and the contacting areas between melting fluxes and aluminum droplets are increased under identical conditions when the diameters of the aluminum droplets are decreased. The inclusions can not be removed effectively by the conventional method of flux purifying because the long-range mass transfer of the inclusions can be restricted, and the aluminum droplet dispersion decreases diffusion length of the inclusions in the molten aluminum. Moreover, the rising rotary motion of the aluminum droplets increases the mass transfer coefficient of the inclusion, which is increased by the rotating speed of the agitor.

In addition, the contact area between the aluminum droplet and the flux is increased when the molten aluminum is dispersed into fine aluminum droplets in stirring melting flux, and contacting area is in direct proportion to $(N^3 D^2)^{0.4}$ advanced by Chen and Middleman[27].

The molten aluminum is dispersed as the fine aluminum droplets by rotary melting flux, and the fine aluminum droplets are aggregated and dispersed repeatedly. Thus the inclusions in molten aluminum can be distributed on the surface of aluminum droplets. On the other hand, the surfaces of aluminum droplet and melting flux are renewed continuously in that aluminum droplets are in rotary melting flux, and the inclusions in aluminum droplets are distributed renewedly and transferred onto the surface of aluminum droplet. This may avoid the long-range mass transfer of the inclusion due to the limitation of viscosity and tension force of the molten aluminum. In addition, the molten aluminum is dispersed as the fine aluminum droplets continuously with the increase of purification times, and the inclusions are distributed ceaselessly on the surface of the aluminum droplets. Moreover, the interface area between the aluminum droplet and the flux is increased when the molten aluminum is dispersed into finer aluminum droplets in stirred melting flux. Hence, the probability for the inclusions transferred into the melting flux is increased. Meanwhile, the thickness of the aluminum film on the surface of the inclusion is worn down, and the inclusions can easily pass through interface between the aluminum liquid and the flux and enter the stirred molten flux. So, the inclusions in molten aluminum are removed efficiently using the method of stirred molten flux purification.

4.3 Analysis of experimental results

The molten aluminum is dispersed into fine aluminum droplets under shear force when the molten aluminum is poured into the rotary melting flux in batches. The aluminum droplets pass through the layer of the rotary melting flux and sink to the graphite crucible bottom because the density of molten aluminum is larger than that of melting flux. The fine aluminum droplets are covered by the film of molten flux to prevent the aluminum droplets

from reacting with $H_2O(g)$ and O_2, so that the second oxidation can not occur. In addition, the thickness of molten flux is enough to prevent rotary molten aluminum from spraying out of the molten flux layer and contacting the air.

Table 2 indicates that the increase of tensile strength and the slight decrease of elongation percentage of tensile samples result from various effects. Though the content of inclusions in the molten aluminum is low, and partially removing the inclusions by stirring melting flux can decrease the amount of tiny crack sources. As a consequence the tensile strength is increased and the elongation percentage is improved. However, the elements of the molten flux enter the molten aluminum and can dissolve in the metal after solidification according to phase diagram. Moreover, the elements in solid solution induce distortion of lattice of aluminum and pin up dislocation, which restrains the immigration of the gliding plane and leads to rigidification. Therefore, the elongation percentage is decreased slightly and the tensile strength is increased[28].

SEM photographs of tensile sample S_0 unpurified by the active melting flux show that some inclusions and pinholes exist at the site of fracture, which leads to partial stress concentration in the fracture and easily produces brittle fracture. Besides, SEM photograph shows that purified tensile sample S_4 makes the ductile rupture happen[29] because stirring molten active flux removes most of the inclusions and pinholes in molten aluminum.

The inclusion quantity and size of tensile sample S4 are fewer and smaller than those of tensile sample S_0 according to the Leco image analytic software statistics and metallographs. Therefore, most of the inclusions in molten aluminum are removed by stirring molten flux.

5 CONCLUSIONS

1) The active flux can chemically react with the inclusions in the molten aluminum.

2) Most of the inclusions in the molten aluminum can be removed with stirring active melting flux, and the tensile strength is increased by 8.59%.

3) The inclusions tend to transfer from the molten aluminum to molten active flux according to thermodynamic analysis.

4) The volume fraction of the inclusions in molten aluminum is reduced from 1.23% to 0.92% after molten aluminum purified by stirring molten active flux, which may change fracture process of casting and improve material performance.

5) The inclusions can easily transfer into molten active flux by stirring molten flux process according to surface renewal kinetic model.

REFERENCES

[1] LI Tiarxiao, SUN Baorde, XU Zherming. A new method of purifying aluminum alloyrinclusion conglomeration[J]. Materrial science & Technology, 1999, 7(3): 30 - 35. (in Chinese)

[2] QIU Zhurxian. Aluminum Electrolysis[M]. Beijing: Metallurgical Industry Press, 1986. 339 - 353. (in Chinese)

[3] FU Gaorshe, KANG Jirxing. Study on the purification of Al scraps by flux filtration[J]. Special Casting & Nonferrous Alloys, 1996, 84(3): 12 - 14. (in Chinese)

[4] FU Gaorshe, KANG Jirxing. The research of waste aluminum purified and filtered with active flux[J]. Special Casting & Nonferrous Alloys, 1996, 84(5): 19~ 22. (in Chinese)

[5] FU Gaorshe, KANG Jirxing. The research of industrial pure aluminum highrefficiently purified with flux[J]. Special Casting & Nonferrous Alloys, 1998, 96(1): 73~ 77. (in Chinese)

[6] FU Gaorshe, KANG Jirxing, Chen Werrzhe, et al. The industrial pure aluminum purified and filtered by Highrefficient flux[J]. The Chinese Journal of Nonferrous Metals, 2000, 10(3): 433 - 436. (in Chinese)

[7] FU Gaorshe, KANG Jirxing. Study of Highrefficient flux of purification used in commercial purity aluminum and its effect of purification[J]. Journal of Fuzhou University(Natural Science), 1998, 26(1): 73 - 77. (in Chinese)

[8] Sahai Y. Role of molten salts in secondary remelting of aluminum scrap[A]. Australian, Asian, Pacific Course and Conference on Aluminum Cast House Technology: Theory and Practice[C]. Minerals, Metals & Materials Soc(TMS), 1993, 4(8): 265.

[9] Sorrel J G, Groetsch Jr. Subsolidus compatibility in the system NaCl-KCl-$AlCl_3$-NaF-KF-AlF_3[J]. Journal of the American Ceramic Society, 1986, 69(4): 333 - 338.

[10] Crepeau P N, Schneider, Wolfgang, et al. Solid fluxing practices for aluminum melting[J]. Modern Casting, 1992(7): 28 - 30.

[11] Utigard T A, Friesen K, Roy R R, et al. The properties and uses of fluxes in molten aluminum processing[J]. JOM, 1998(11): 38 - 41.

[12] Cochran B P, Richard P, Edward D, et al. Flux practice in aluminum melting[J]. AFS Transaction, 1992, 92 - 88: 737 - 742.

[13] Ho F K, Sahai Y. Interfacial tension in molten aluminum and salt systems[A]. Light Metals: Proceedings of Sessions[C]. TMS Annual Meeting(Warrendale, Pennsylvania), 1993, 21 - 25. Publ by Minerals, Metals & Materials Soc(TMS). 1067 - 1072.

[14] Beckett B. Role of modern salt baths in processing of aluminium and its alloys[A]. Aluminium Technology'86, Proceedings of the International Conference. 1986 Sponsored by: Inst of Metals, Metals Technology Committee[C]. London: Engl; Assoc Italiana di Metallurgia, Italy; ASM, Metals Park, OH, USA; Japan Inst of Metals, Jpn; Norsk Metallurgisk Selskap, Norw; Soc Francaise de Metallurgie, Fr

Inst of Metals, 789 - 793.

[15] Kogan M H. Dross Processing at Commonwealth Aluminum Plant[M]. American Foundrymen's Society, Iliinois, 1989. 251 - 263.

[16] LI Jing, HUANG Ke-xiong, WANG Zao-ji, et al. The research of the interface phenomenon among aluminum liquid-molten salt-electrode[J]. Acta Metallurgica Sinica, 1990, 26(1): 6~ 10. (in Chinese)

[17] FU Gao-she, KANG Ji-xing. Analysis on the characters of purification in molten aluminum[J]. Foundry Technology, 1995, 84(6): 23~ 26. (in Chinese)

[18] Bruce M D, Taghiei M M. Interfacial reactions between aluminum alloys and salt flux during melting[J]. Materials Transaction, JIM, 1989, 30(6): 411 - 422.

[19] Shell D J, Nilmani M, Fox M H, et al. Aluminium dross treatment using salt fluxes[A]. Proceedings of the 4th Australasian Asian Pacific Conference on Aluminium Cast House Technology[C], 1995. 3 - 6. Minerals, Metals & Materials Soc(TMS), 1995. 133.

[20] Apelian D, Luk S, Piccone T, et al. Fifth international iron and steel congress[A]. Proceedings of the 69th Steel Making Conference[C]. 1986, 69: 957 - 967.

[21] Lida T, Guthrie R. Mass Transfer and Absorbers[M]. Oxford: Clarendon Press, 1993. 188.

[22] Danckwerts P V. Significance of liquid-film coefficients in gas absorption[J]. Industrial and Engineering Chemistry, 1951, 43: 1460 - 1467.

[23] XIA Guang-rong, HONG Quan-li. Transferring Similarity [M]. Beijing: China Petrochemical Industry Press, 1997. 7 - 10. (in Chinese)

[24] ZHOU De-zheng. Mass Transfer and New Style Turricula Equipment[M]. Chongqing: Chongqin University Press, 1991. 67 - 89. (in Chinese)

[25] MO Ding-chen. Metallurgic Kinetics[M]. Changsha: Central South University Technology Press, 1984. 139 - 157. (in Chinese)

[26] Olander D R. Simultaneous mass transfer and chemical reaction[J]. A I Ch E J, 1960, 5: 293 - 300.

[27] Chen H T, Middleman S. Drop size distribution in agitated liquid-liquid systems[J]. A I Ch E J, 1967, 13(5): 989 - 996.

[28] WANG Zhu-tang, ZHANG Zhen-lu, ZHEN Xuan. Aluminum Alloy Texture and Performance[M]. Beijing: Metallurgical Industry Press, 1985. 170 - 177. (in Chinese)

[29] Henry G, Horstmann D. Macroscopical Fracture and Microfracture[M]. Beijing: Mechanical Industry Press, 1987. 5 - 20. (in Chinese)

(Edited by PENG Chao-qun)